URSI GASS 2020, Rome, Italy, 29 August - 5 September 2020

Investigation of Time-Averaged Poynting Localized Energy Dynamics around Narrowband and Ultrawideband Antenna Systems

Debdeep Sarkar(1), Said Mikki(2), and Yahia Antar(1)
(1) Department of Electrical and Computer Engineering, Royal Military College of Canada, Kingston, ON, Canada
(2) Department of Electrical and Computer Engineering, University of New Haven, West Haven, CT, USA

Abstract

In this paper, we investigate the spatial dynamics of the recently discovered time-averaged Poynting localized energy around antennas using a finite-difference time-domain (FDTD) analysis technique. We consider two-port antenna systems comprised of: (i) narrowband thin-wire dipoles and (ii) ultrawideband (UWB) "fat" dipoles based on circular patches. Using FDTD, we characterize the S-parameters as well as evaluate the time-averaged localized energy distribution along an observation plane for differentiated Gaussian pulse excitation. Full-wave simulation results provide critical insight into *energy signature manipulation* in regions between closely spaced UWB antennas by changing their relative orientations. It is found that significant departure from S-parameters-based insights is revealed in the new localized energy data generated here using our method with practical antenna types as examples.

1 Introduction

The subject of non-propagating energy content around antennas in general has found significant attention in the applied electromagnetics community, especially emphasizing upon the antenna stored-energy and quality-factor (Q-factor) [1]-[5]. The reliance on circuit-theoretic approach and antenna Q-factor has indeed some engineering importance in the context of impedance matching of electrically small antennas (ESAs) [3],[5]. But in the present digital age where one strives for high data-rates for pulse-like impulse streams, it is critical to look into the minute details of the near-zone non-propagating energy for non-resonant ultra-wideband (UWB) antennas [6]-[7], something that is not covered in the purview of the traditional Q-factor/reactive energy approach[1]. Interestingly, the authors in [4] mention the requirement to explore "new possibilities for analyzing radiators in the time domain, namely the ultra-wideband radiators and other systems working in the pulse regime." In [10], a new look into the spatial structure of the antenna near-field is provided by adopting Wilcox-expansion approach [11]. Also the extremely vital distinctions between antenna near-field energy types like "reactive energy", "localized energy" and "recoverable energy" are highlighted in [9],[10]. In [12], a computational paradigm for estimating time-domain reactive energy around arbitrary antennas, is developed by integrating finite-difference time-domain (FDTD) and infinitesimal dipole modelling (IDM) methods.

In [13], the concept of Poynting localized energy around antennas, fundamentally different from the traditional antenna reactive energy, was introduced for the first time[2]. The computation time-domain reactive energy requires infinitesimal dipole modelling (IDM) of radiating antenna currents, implying that the accuracy of the method depends on proper utilization of suitable equivalence principles [12]. But the Poynting localized energy approach does not deal with any such radiating current approximation, and directly works with the local *interpolated* electric and magnetic fields generated by FDTD time-marching (see [15] for details), thereby making the computation more robust as compared to the FDTD-IDM approach. In [16]-[18], we demonstrated the usefulness of Poynting localized energy approach in observing the energy dynamics around slot-loaded printed dipoles or pattern-reconfigurable antennas, and also predicting gain-enhancement in strongly coupled antenna systems (eg. Yagi-Uda arrays). In this paper, we study the Poynting localized energy aspects for both narrow-band and UWB MIMO antennas, and delve deeper into the mutual coupling/energy-exchange aspects.

2 Numerical Example and Results

2.1 Narrow-band System Analysis

We start our analysis with a system of two narrow-band center-fed dipoles (see Fig. 1(a)). Each dipole has length L_1 and are separated by distance a d. The FDTD simulation setup under consideration has cubical spatial grids with $\Delta x = \Delta y = \Delta z = \Delta = 1$ mm and time-stepping $\Delta t = 1.533$ ps [12],[18]. To first obtain the S-parameter magnitude response ($|S_{11}|$ and $|S_{21}|$) as well as the spatial map of localized energy (i.e. $\bar{W}_{\text{loc}}(x,y,z)$) later on, we use a differenti-

[1] However, it is important to note here that the underlying ideas of enabling transmission of high-information-rate signal using a "narrow-band" or high Q-factor antennas, are described in [8] from an energy balance and thermodynamic point of view

[2] Note that the Poynting localized energy is also different from Kaiser's "relativistic" inertial energy around radiators, which he calls "reactive energy" (see [14]).

ated Gaussian pulse $v_{dg}(t)$ for exciting the dipoles:

$$v_{dg}(t) = A_1(t-t_1)e^{-(t-t_1)^2/\sigma_1^2} \quad (1)$$

where pulse-launch time $t_1 = 50\Delta t$ and spread is $\sigma_1 = 5\Delta t$. The total FDTD transient simulation runs for the time $T_{max} = 1200\Delta t$. The simulated S-parameters in Fig. 1(b) indicate that the dipoles have impedance matching point ($|S_{11}| = -13.58$ dB) at $f_0 = 2.94$ GHz, indicating the fundamental half-wavelength mode of dipole operation (i.e. $L_1 \approx 0.48\lambda_0$).

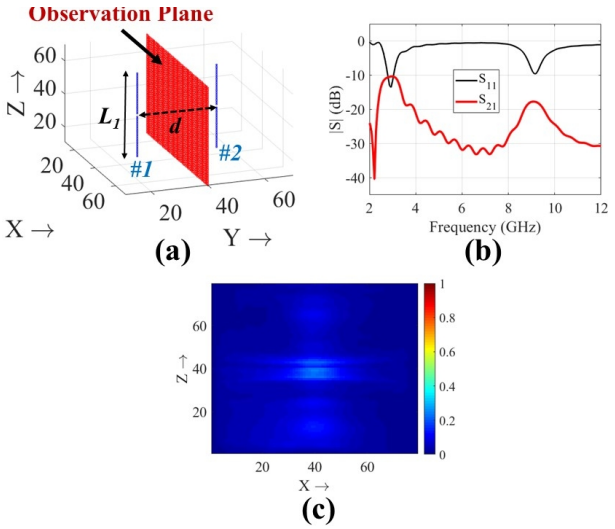

Figure 1. (a) FDTD simulation setup of a system of two thin-wire dipoles in free-space with design parameters $L_1 = 49\Delta$ and $d = 28\Delta$, where $\Delta = 1$mm is the FDTD cubic grid size. (b) Corresponding frequency responses of simulated $|S_{11}|$ and $|S_{21}|$. (c) Normalized localized energy signature $\bar{W}_{loc}(x,y,z)$ for this two-dipole system on the observation region (see (a)) of interest along xz-plane. Note that, we consider dipole-1 to be excited by $v_{dg}(t)$ (see (1)), while keeping dipole-2 in matched load termination.

Also the port-to-port mutual coupling at this frequency is $|S_{21}| = -10.38$ dB, and strongly depends on the spacing d as shown in Fig. 1(a). As we are analysing the system for a broadband excitation pulse, one anticipated higher order harmonic response is observed at 9.13 GHz. Fig. 1(c) shows the corresponding normalized spatial-map of time-averaged Poynting localized energy $\bar{W}_{loc}(x,y,z)$ along the plane $y = y_0$, exactly mid-way between the two working dipoles and indicated by the red-region. Note that, we would use the same constant to normalize the spatial energy plots for analyzing the UWB systems next.

2.2 UWB System Analysis

As shown in Fig. 2(a), we transform the two arms of the thin-wire dipoles (Fig. 1(a)) into circular patches having radius $\approx 0.25L_1$. It is well known in UWB antenna community (see [**?**]) that such a "fat-dipole" would inherently lead to wider impedance matching bandwidth[3]. We consider various two-antenna configurations based on the relative orientation of these circular patches along the xz and yz-planes (see Fig. 2). Note that, for all the structures Case-I to Case-IV as shown in Fig. 2, we keep separation between individual dipole feed-points the same, but vary the edge-to-edge separation. In the final structure Case-IV (see Fig. 2(d)), the individual dipole arms are realized by a combination of two mutually orthogonal circular patches, essentially leading two a three-dimensional dipole structure. Fig. 3(a) demonstrates that this Case-IV configuration provides the best performance in terms of impedance matching bandwidth, by providing $|S_{11}| < -10$ dB over the popular UWB operating regime ($3.1 - 10.6$ GHz).

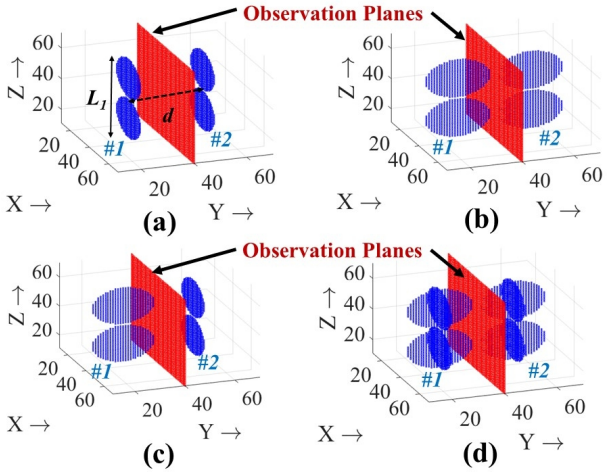

Figure 2. FDTD simulation setup for four possible relative orientations of fat UWB dipoles: (a) Case-I, (b) Case-II, (c) Case-III and (d) Case-IV. Note that the UWB dipoles have same design parameters L_1 and d for the narrowband dipoles in Fig. 1(a).

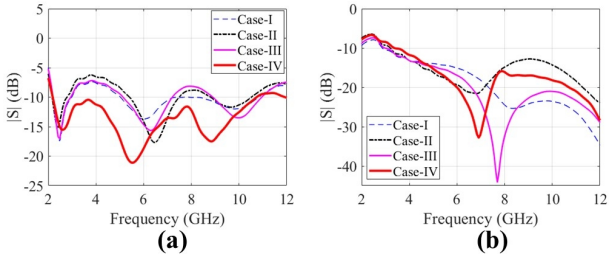

Figure 3. Comparison of simulated frequency responses of: (a) $|S_{11}|$ and (b) $|S_{21}|$, for the four configurations shown in Fig. 2.

Next we critically observe the broadband $|S_{21}|$ response for the the strongly resonant two-dipole system of Fig. 1(a) and the UWB dipole systems of Fig. 2, and make some comments about the mutual coupling and energy exchange, when short-duration Gaussian pulses are used as excitation

[3] In this work, we are not interested in design of impedance-matching Baluns or wide-band tapered sections for feeding purpose. Our main focus is on exploring the fundamental radiation, energy localization and coupling issues, therefore we use simple Delta feed-gap based excitation scheme for the UWB dipoles too.

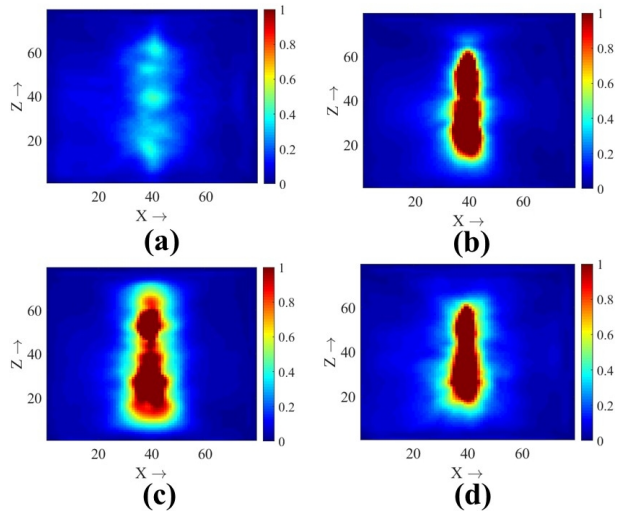

Figure 4. Normalized localized energy signature $\bar{W}_{\rm loc}(x,y,z)$ for the two UWB dipole system of Fig. 2 along the observation xz-plane of interest: (a) Case-I, (b) Case-II, (c) Case-III and (d) Case-IV. Similar to Fig. 1, in order to compute $\bar{W}_{\rm loc}$, we excite the dipole-1 by $v_{\rm dg}(t)$ and terminate the other UWB-dipole by matched load termination.

signal. For the two-dipole configuration of Fig. 1(a), the port-to-port mutual coupling is significant only in the narrow working bands around 3 GHz and 9 GHz (see Fig. 1(b)). When this narrowband system is excited by a short-duration (i.e. wide-band) pulse like $v_{\rm dg}(t)$, the $\bar{W}_{\rm loc}(x,y_0,z)$ plots are considerably weak. However on the other hand, the UWB dipole system of Fig. 2(a), bearing the same center-to-center and edge-to-edge physical separation as the narrow-band dipole system in Fig. 1(a), has *increased* port-to-port mutual coupling (i.e. $|S_{21}|$) over the wide frequency bandwidth (see Case-I, Fig. 3(b)). Note that, we make this comparison in the "average" sense by estimating $\int_{f_1}^{f_2}|S_{21}(f)|df$, where the observation frequency range is f_1 to f_2. One can say that the UWB-dipoles accept the energy content of the wide-band temporal excitation pulse, and radiate it over space-time more effectively, resulting in the enhanced $\bar{W}_{\rm loc}(x,y_0,z)$ response along the observation plane (see Fig. 4(a)), compared to the narrow-band dipole system.

When at least one UWB dipole in the two-element system is oriented along the yz-plane, i.e. for Case-II to Case-IV (Fig. 2(b) to Fig. 2(d)), the observation plane is in close proximity with the dipole edges. This naturally enhances the localized energy considerably as compared to the "face-to-face" orientation (Fig. 2(a)), which is reflected in general from the strong "hot-spot" like features in $\bar{W}_{\rm loc}(x,y_0,z)$ plots from Fig. 4(b) to Fig. 4(d). It is evident that there are significant differences between Fig. 4(b) and Fig. 4(c), which are the $\bar{W}_{\rm loc}(x,y_0,z)$ plots along the observation plane for respectively the "side-by-side" (Fig. 2(b)) and "mutually orthogonal" (Fig. 2(c)) orientations of the UWB dipoles. A quick comparison between Fig. 4(b) and Fig. 4(d) also demonstrates the tailoring of spatial localized energy responses caused by embedding of the circular patches on dipole arms, although the overall "volume" circumscribing the two-antenna configuration remains unchanged (see Fig. 2(b) and Fig. 2(d)).

3 Conclusions

In this paper, we studied the spatial patterns of time-averaged Poynting localized energy around two-port antenna systems comprised of either narrow-band or UWB dipoles. Employing an in-house FDTD methodology, we specifically demonstrated that the spatial distribution (or "pattern") of time-averaged near-zone localized energy is considerably *shaped* by either the relative antenna-orientations or by modifications on the radiating structure topology. This appears to happen even though the traditional reflection coefficient (i.e. $|S_{11}|$) or port-to-port mutual coupling (i.e. $|S_{21}|$) responses may not be dramatically different. Note that, the time-domain antenna reactive energy computed via FDTD-IDM principle (see [12]) does not provide any spatial features or patterns, in contrast to the proposed Poynting localized energy approach which seems to reflect hidden feature in the antenna system overlooked in previous investigations. It is anticipated that such observations pertaining to Poynting localized energy distributions will become critical for the optimal design of highly-directive wireless devices, efficient energy harvesting systems, and distributed sensor-nodes having several antennas packed within a compact volume.

References

[1] V. N. Kessenikh, "Bound Energy of Radiating Wires," *Zhurnal Tekhnicheskoi Fiziki* (in Russian), **9**, 17, 1939, pp. 1557–1563.

[2] R. E. Collin and S. Rothschild, "Evaluation of Antenna Q," *IEEE Transactions on Antennas and Propagation*, **12**, 1964, pp. 23–27.

[3] W. Geyi, "A Method for the Evaluation of Small Antenna Q," *IEEE Transactions on Antennas and Propagation*, **51**, 8, 2003, pp. 2124–2129.

[4] M. Capek, L. Jelinek., and G. A. E. Vandenbosch, "Stored Electromagnetic Energy and Quality Factor of Radiating Structures," *Proceedings of the Royal Society A*, **472**, 2188, April 2016, doi: 10.1098/rspa.2015.0870.

[5] K. Schab, L. Jelinek, M. Capek, C. Ehrenborg, D. Tayli, G. A. E. Vandenbosch, and M. Gustafsson, "Energy Stored by Radiating Systems," *IEEE Acess*, **6**, 2018, 10553–10568.

[6] B. A. Kramer, C. C. Chen, M. Lee and J. L. Volakis, "Fundamental Limits and Design Guidelines for Miniaturizing Ultra-Wideband Antennas," *IEEE Antennas and Propagation Magazine*, **51**, 4, 2009, pp. 57–69.

[7] C. Saha, J. Y. Siddiqui and Y. M. M. Antar, *Multifunctional Ultrawideband Antennas Trends, Techniques and Applications*, CRC Press, Taylor and Francis, 2019.

[8] M. Manteghi, "Fundamental Limits, Bandwidth, and Information Rate of Electrically Small Antennas: Increasing the Throughput of an Antenna Without Violating the Thermodynamic Q-Factor," *IEEE Antennas and Propagation Magazine*, **61**, 3, June 2019, pp. 14-26.

[9] S. M. Mikki and Y. M. M. Antar, "A New Technique for the Analysis of Energy Coupling and Exchange in General Antenna Systems," *IEEE Transactions on Antennas and Propagation*, vol. 63, no. 12, pp. 5536-5547, Dec. 2015.

[10] S. Mikki and Y. M. M. Antar, *New Foundations for Applied Electromagnetics: Spatial Structures of Electromagnetic Field*, Norwood, MA, USA: Artech House, 2016.

[11] C. H. Wilcox, "An Expansion Theorem for Electromagnetic Fields," *Communications on Pure and Applied Mathematics (Wiley)*, 1956, pp. 115–134.

[12] D. Sarkar, S. Mikki, K. V. Srivastava and Y. M. M. Antar, "Dynamics of Antenna Reactive Energy Using Time Domain IDM Method," *IEEE Transactions on Antennas and Propagation*, **67**, 2, 2019, pp. 1084–1093.

[13] S. Mikki, D. Sarkar and Y. M. M. Antar, "On Localized Antenna Energy in Electromagnetic Radiation," *Progress in Electromagnetics Research (PIER) M*, **79**, 2019, pp. 1–10.

[14] G. Kaiser, "Conservation of Reactive EM energy in Reactive time," *Proceedings of 2015 IEEE International Symposium on Antennas and Propagation and USNC/URSI National Radio Science Meeting (APSURSI)*, 2015, pp. 1704–1705.

[15] R. Kastner and O. Asaf, "Energy Conservation and Poynting's Theorem in the Staggered FDTD Grid," *Proceedings of URSI General Assembly, Chicago,* 2008, pp. 1–4.

[16] D. Sarkar, Y. Antar and S. Mikki, "Consideration of Poynting Localized Energy Around Radiators: An FDTD-based Investigation," *2019 IEEE International Symposium on Antennas and Propagation and USNC-URSI Radio Science Meeting*, Atlanta, GA, USA, 2019, pp. 1665–1666, doi: 10.1109/APUSNCURSINRSM.2019.8888611.

[17] D. Sarkar, S. Mikki and Y. M. M. Antar, "Spacetime Analysis of Energy Localization: A Poynting Flow Perspective With Applications to Pattern Reconfigurable Dipoles," *International Journal of RF and Microwave Computer-Aided Engineering (Wiley)*, 29:e21920, November 2019, pp. 1–11.

[18] D. Sarkar, S. Mikki and Y. M. M. Antar, "Poynting Localized Energy: Method and Applications to Gain Enhancement in Coupled Antenna Systems," *IEEE Transactions on Antennas and Propagation*, 2020. (In Press)

[19] J. Diao, L. Liu and K. F. Warnick, "An Intuitive Way to Understand Mutual Coupling Effects in Antenna Arrays Using the Poynting Streamline Method," *IEEE Transactions on Antennas and Propagation*, **67**, 2, 2019, pp. 884–891.